Diffusion-induced bending of viscoelastic beams

Fuqian Yang
Department of Chemical and Materials Engineering
University of Kentucky, Lexington, KY 40506
fyang2@uky.edu

Abstract

The contribution of local volumetric change due to the diffusion/migration of solute atoms to viscoelastic deformation is incorporated in the theory of linear viscoelasticity, following the elastic theory of diffusion-induced stress. Three-dimensional constitutive relationship in differential form for diffusion-induced stress in linear viscoelastic materials is proposed. Using the correspondence principle between linear viscoelasticity and linear elasticity and the results from the diffusion-induced bending of elastic beams, the radii of curvature of the centroidal plane of viscoelastic beams of single layer and bilayer with top layer being viscoelastic in the transform domain are obtained. For viscoelastic beams of single layer, closed-form solution of the radius of curvature of the centroidal plane is derived, and the radius of curvature is inversely proportional to the diffusion moment created by non-uniform distribution of solute atoms. For the condition of constant concentration on free surface, there is overshoot behavior; for the condition of constant flux on free surface, there is no overshoot behavior. For viscoelastic beams of bilayer with top layer being the Maxwell-type standard material, the numerical results show the presence of the overshoot behavior for very compliant elastic layer under the condition of constant concentration on free surface, and there is no overshoot behavior under the condition of constant flux on free surface.

Keywords: Diffusion-induced stress; bending; viscoelastic beam.

1. Introduction

The progress in the micro- and nanomanufacturing technologies has made it possible to manufacture cantilever-based structures for sensing techniques [1-5]. Similar structures, beam-based structures, have also been used to analyze the change of surface stress due to electrochemical charging-discharging [6-10] and the stresses induced by mass transport [7, 11-15]. In the heart of the cantilever-based sensing techniques is the change of surface stress associated with adsorption of molecules on "active" surface/coating and/or the volumetric strain associated with phase change and/or mass transport, which can cause the deflection of the cantilever-based structures.

Currently, the deflection analysis of cantilever-based structures and beam-based structures has mainly based on the theory of elastic beams with the incorporation of surface stress and the strain due to swelling/shrinking of coated materials. It is known that polymer coatings have been used in cantilever-based chemical sensors [9, 12, 15]. The theory of elastic beams likely cannot reveal the temporal evolution of the beam deflection with a coating of polymer. For example, Pei and Inganäs [13] used the theory of linear elasticity to model the deflection of a bipolymer strip induced by cation insertion and salt draining, and stated that their numerical results may not compare with the experimental results of the increasing part of the bipolymer strip deflection. They suggested that this is likely due to the salt draining occurring immediately after the reduction. Observing an overshoot that slowly decreases to the steady-state value for the absorption of a chemical analyte into a polymer coating, Wenzel et al. [16] developed a model of absorption-induced static bending of a microcantilever coated with a viscoelastic material, and were able to demonstrate the overshoot behavior from their model. It is worth mentioning that Yang and Li [17] used the elastic theory of diffusion-induced stress to analyze the cantilever-based hydrogen sensor, and their results showed the overshoot behavior. Yang [18] used the theory of surface rheology to analyze the effect of a surface viscous film on the vibration of an elastic microcantilever. Approximating uniform temperature in a bilayer system, Hsueh et al. [19] used the correspondence principle to analyze the stress evolution in the bilayer consisting of Maxwell materials due to thermal and/or lattice mismatch. They did not analyze the temporal evolution of the radius of curvature of the viscoelastic bilayer system. There are little studies focusing on the diffusion-induced bending of cantilever-based structures consisting of viscoelastic materials.

It is known that polymer coatings have been widely used in cantilever-based sensing structures and conducting polymer as well as porous materials has bee used in energy storage such as

supercapacitors [20-24]. There exists local volumetric change associated with mass transport and phase transform in polymer and porous materials, and it needs to carefully study the effect of the volumetric strain on the structural sensetivity for the applications in sensing technology and energy storage. Considering the viscoelastic characteristcs of polymer and porou materials associated with fluid-structure interaction, the effect of the volumetric strain due to mass transport on the bending of viscoelastic beams is analyzed. The focuse is on the temporal evolution of the beam deflection. The theory of diffusion-induced stress in linear elasticity is extended to linear viscoelasticity.

2. Analyses of diffusion-induced bending of elastic beams

In the framework of linear elasticity, the constitutive relationship describing the diffusion-induced deformation of elastic materials is [25]

$$\boldsymbol{\varepsilon} = \frac{1}{E}[(1+\nu)\boldsymbol{\sigma} - \nu \mathrm{tr}(\boldsymbol{\sigma})\mathbf{I}] + \frac{c\Omega}{3}\mathbf{I} \tag{1}$$

where $\boldsymbol{\varepsilon}$ is strain tensor, $\boldsymbol{\sigma}$ is stress tensor, $\mathbf{I}$ is unit tensor, Ω is the molar volume of solute atoms (m^3/mol), c is the concentration (mol/m^3) of diffusing component (solute atoms), and E and ν are Young's modulus and Poisson's ratio of the material, respectively. The molar volume of Ω is assumed constant, independent of c. The relationship between the strain tensor and the displacement vector ($\boldsymbol{u}$) is

$$\boldsymbol{\varepsilon} = \frac{1}{2}\left(\nabla \boldsymbol{u} + \boldsymbol{u}\nabla\right) \tag{2}$$

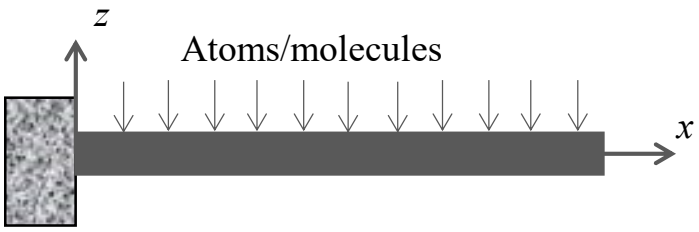

Figure 1. Schematic diagram of the diffusion/migration of atoms/molecules into an elastic beam of single layer

Figure 1 shows an elastic beam with the dimensions in the y- and z-directions much smaller than that in the x-direction. Equation (1) reduces to

$$\varepsilon_{xx} = \frac{1}{E}\sigma_{xx} + \frac{c\Omega}{3} \tag{3}$$

for the diffusion-induced bending of the elastic beam.

Elastic beam of single layer

For completeness, the diffusion-induced bending of an elastic beam of Young's modulus of E_1 with the dimensions in the *y*- and *z*-directions much smaller than that in the *x*-direction is first briefly analyzed. For detailed derivation, see the work by Yang and Li [17]. According to the Bernoulli–Euler assumption that planar sections perpendicular to the axis remain planar after bending, one can express axial displacement (*x*-direction), $u(x, z)$, as

$$u(x,z) = f_0(x) + zf_1(x) \tag{4}$$

From Eq. (4), the axial normal strain, ε_{xx}, and stress, σ_{xx}, can calculated as

$$\varepsilon_{xx}(x,z) = f_0^{'}(x) + zf_1^{'}(x) \tag{5}$$

$$\sigma_{xx}(x,z) = E_1[f_0^{'}(x) + zf_1^{'}(x) - \frac{1}{3}c\Omega] \tag{6}$$

Here, $f_0(x)$ and $f_1(x)$ are to be determined from the equilibrium equations, and the primes denote differentiation with respect to *x*.

Assuming that the characteristic time for diffusion/migration of solute atoms into the elastic beam is much larger than the characteristic time for the propagation of elastic wave, one can approximate the deflection of the elastic beam as quasi-static. Under the condition of quasi-static state, the equilibrium equations are

$$\int_{A_1} \sigma_{xx}(x,z)dA = 0 \text{ and } \int_{A_1} z\sigma_{xx}(x,z)dA = 0 \tag{7}$$

where the integrations must cover the entire cross-sectional area of A_1.

Substituting Eq. (6) into Eq. (7) and using the condition of $\int_{A_1} zdA = 0$ (i.e. the centroidal plane is the middle plane of the elastic beam) yield

$$f_0^{'}(x) = \frac{1}{3} < c > \Omega \text{ and } f_1^{'}(x) = \frac{1}{3I_1} M_c\Omega \tag{8}$$

with

$$< c >= \frac{1}{A_1}\int_{A_1} cdA,\ M_c = \int_{A_1} czdA, \text{ and } I_1 = \int_{A_1} z^2 dA \tag{9}$$

Here, M_c is defined as diffusion moment. Substituting Eq. (8) into Eqs. (5) and (6), one obtains the strain and stress in the elastic beam as

$$\varepsilon_{xx}(x,z) = \frac{1}{3} < c > \Omega + \frac{1}{3I_1} zM_c\Omega \tag{10}$$

$$\sigma_{xx}(x,z)=\frac{E_1\Omega}{3}[(<c>-c)+\frac{z}{I_1}M_c] \tag{11}$$

which gives the radius of curvature, ρ, of the centroidal plane as

$$\frac{1}{\rho}=-\frac{\partial\varepsilon_{xx}(x,z)}{\partial z}=-\frac{1}{3I_1}M_c\Omega \tag{12}$$

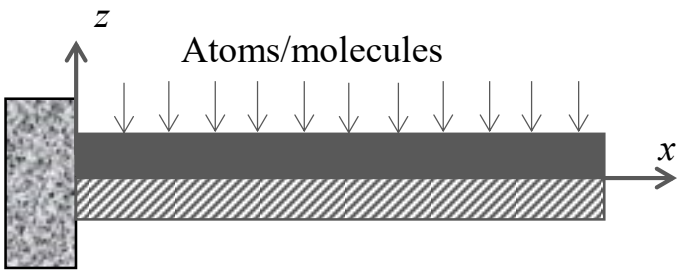

Figure 2. Schematic diagram of the diffusion/migration of atoms/molecules into an elastic beam of bilayer

Elastic beam of bilayer

Consider an elastic beam consisting of two elastic layers with solute atoms only being able to migrate/diffuse into top layer, as shown in Fig. 2. There is perfect bonding between top layer and bottom layer, and there is no slip between these two layers. The elastic moduli are E_1 and E_2 for the top layer and the bottom layer, respectively.

Similar to the analysis of the bending of the elastic beam of single layer, the axial displacement (x-direction), $u(x, z)$, can be expressed as

$$u(x,z)=f_0(x)+zf_1(x) \tag{13}$$

in which the x-axis (z=0) is located in the interface between the top layer and the bottom layer. The axial strains of each layer can then be calculated as

$$\frac{\sigma_{xx1}}{E_1}=\varepsilon_{xx1}-\frac{1}{3}c\Omega=f_0^{'}(x)+zf_1^{'}(x)-\frac{1}{3}c\Omega \qquad \text{for top layer} \tag{14}$$

$$\frac{\sigma_{xx}}{E_2}=\varepsilon_{xx2}=f_0^{'}(x)+zf_1^{'}(x) \qquad \text{for bottom layer} \tag{15}$$

Without the action of external loading, the equilibrium equations give

$$\int_{A_1}\sigma_{xx_1}(x,z)dA+\int_{A_2}\sigma_{xx_2}(x,z)dA=0 \tag{16}$$

$$\int_{A_1}z\sigma_{xx_1}(x,z)dA+\int_{A_2}z\sigma_{xx_2}(x,z)dA=0 \tag{17}$$

Here, A_1 and A_2 are the cross-sectional areas of the top layer and the bottom layer, respectively. Substituting Eqs. (14) and (15) into Eqs. (16) and (17) yields

$$f_0^{'}(x)=\frac{\Omega E_1}{3}\begin{vmatrix} A_1<c> & E_1J_1+E_2J_2 \\ M_c & E_1I_1+E_2I_2 \end{vmatrix}\begin{vmatrix} E_1A_1+E_2A_2 & E_1J_1+E_2J_2 \\ E_1J_1+E_2J_2 & E_1I_1+E_2I_2 \end{vmatrix}^{-1} \tag{18}$$

$$f_1^{'}(x)=\frac{\Omega E_1}{3}\begin{vmatrix} E_1A_1+E_2A_2 & A_1<c> \\ E_1J_1+E_2J_2 & M_c \end{vmatrix}\begin{vmatrix} E_1A_1+E_2A_2 & E_1J_1+E_2J_2 \\ E_1J_1+E_2J_2 & E_1I_1+E_2I_2 \end{vmatrix}^{-1} \tag{19}$$

with

$$J_i=\int_{A_i} zdA \ (i=1, 2) \text{ and } I_2=\int_{A_2} z^2dA \tag{20}$$

Using Eqs. (14), (15), (18) and (19), one obtains the stresses in the bilayer structure as

$$\sigma_{xx_1}(x,z)=\frac{\Omega E_1^2}{3}\left(\begin{vmatrix} A_1<c> & E_1J_1+E_2J_2 \\ M_c & E_1I_1+E_2I_2 \end{vmatrix}+z\begin{vmatrix} E_1A_1+E_2A_2 & A_1<c> \\ E_1J_1+E_2J_2 & M_c \end{vmatrix}\right) \tag{21}$$

$$\cdot\begin{vmatrix} E_1A_1+E_2A_2 & E_1J_1+E_2J_2 \\ E_1J_1+E_2J_2 & E_1I_1+E_2I_2 \end{vmatrix}^{-1}-\frac{1}{3}cE_1\Omega \quad \text{for top layer}$$

$$\sigma_{xx_2}(x,z)=\frac{\Omega E_1E_2}{3}\left(\begin{vmatrix} A_1<c> & E_1J_1+E_2J_2 \\ M_c & E_1I_1+E_2I_2 \end{vmatrix}+z\begin{vmatrix} E_1A_1+E_2A_2 & A_1<c> \\ E_1J_1+E_2J_2 & M_c \end{vmatrix}\right) \tag{22}$$

$$\cdot\begin{vmatrix} E_1A_1+E_2A_2 & E_1J_1+E_2J_2 \\ E_1J_1+E_2J_2 & E_1I_1+E_2I_2 \end{vmatrix}^{-1} \quad \text{for bottom layer}$$

and the radius of curvature of the centroidal plane as

$$\frac{1}{\rho}=-\frac{\Omega E_1}{3}\begin{vmatrix} E_1A_1+E_2A_2 & A_1<c> \\ E_1J_1+E_2J_2 & M_c \end{vmatrix}\begin{vmatrix} E_1A_1+E_2A_2 & E_1J_1+E_2J_2 \\ E_1J_1+E_2J_2 & E_1I_1+E_2I_2 \end{vmatrix}^{-1} \tag{23}$$

It is evident that Eqs. (21) and (23) reduce to Eqs. (11) and (12) for A_2=0 and J_1=0 (i.e. $\int_{A_1} zdA=0$ with the centroidal plane being the middle plane of the elastic layer), respectively.

Two limiting cases are discussed below.

Case I: $E_1A_1 << E_2A_2$

Under the condition of $E_1A_1 << E_2A_2$, the stresses in the bilayer structure and the radius of curvature of the centroidal plane to the zeroth-order approximation are

$$\sigma_{xx_1}(x,z)=\frac{\Omega E_1}{3E_2}\left(\begin{vmatrix} A_1<c> & J_2 \\ M_c & I_2 \end{vmatrix}+z\begin{vmatrix} A_2 & A_1<c> \\ J_2 & M_c \end{vmatrix}\right)\cdot\begin{vmatrix} A_2 & J_2 \\ J_2 & I_2 \end{vmatrix}^{-1}-\frac{1}{3}cE_1\Omega \tag{24}$$

for the top layer,

$$\sigma_{xx_2}(x,z)=\frac{\Omega E_1}{3}\left(\begin{vmatrix} A_1<c> & J_2 \\ M_c & I_2 \end{vmatrix}+z\begin{vmatrix} A_2 & A_1<c> \\ J_2 & M_c \end{vmatrix}\right)\cdot\begin{vmatrix} A_2 & J_2 \\ J_2 & I_2 \end{vmatrix}^{-1} \tag{25}$$

for the bottom layer, and

$$\frac{1}{\rho}=-\frac{\Omega E_1}{3E_2}\begin{vmatrix} A_2 & A_1<c> \\ J_2 & M_c \end{vmatrix}\begin{vmatrix} A_2 & J_2 \\ J_2 & I_2 \end{vmatrix}^{-1} \tag{26}$$

The radius of curvature is proportional to the ratio of the modulus of the bottom layer to that of the top layer.

The stresses in the bilayer structure and the radius of curvature of the centroidal plane to the first-order approximation are

$$\sigma_{xx_1}(x,z)=\frac{\Omega E_1^2}{3}\left(\begin{vmatrix} A_1<c> & E_1J_1+E_2J_2 \\ M_c & E_1I_1+E_2I_2 \end{vmatrix}+z\begin{vmatrix} E_1A_1+E_2A_2 & A_1<c> \\ E_1J_1+E_2J_2 & M_c \end{vmatrix}\right) \tag{27}$$

$$\cdot\left(E_1E_2A_1I_2+E_1E_2I_1A_2+E_2E_2A_2I_2-2E_1E_2J_1J_2-E_2^2J_2^2\right)^{-1}-\frac{1}{3}cE_1\Omega$$

for the top layer,

$$\sigma_{xx_2}(x,z)=\frac{\Omega E_1E_2}{3}\left(\begin{vmatrix} A_1<c> & E_1J_1+E_2J_2 \\ M_c & E_1I_1+E_2I_2 \end{vmatrix}+z\begin{vmatrix} E_1A_1+E_2A_2 & A_1<c> \\ E_1J_1+E_2J_2 & M_c \end{vmatrix}\right) \tag{28}$$

$$\cdot\left(E_1E_2A_1I_2+E_1E_2I_1A_2+E_2E_2A_2I_2-2E_1E_2J_1J_2-E_2^2J_2^2\right)^{-1}$$

for the bottom layer, and

$$\frac{1}{\rho}=-\frac{\Omega E_1\left[(E_1A_1+E_2A_2)M_c-A_1<c>(E_1J_1+E_2J_2)\right]}{3\left(E_1E_2A_1I_2+E_1E_2I_1A_2+E_2E_2A_2I_2-2E_1E_2J_1J_2-E_2^2J_2^2\right)} \tag{29}$$

Case II: $E_2A_2 \ll E_1A_1$

Under the condition of $E_2A_2 \ll E_1A_1$, the stresses in the bilayer structure and the radius of curvature of the centroidal plane to the zeroth-order approximation are

$$\sigma_{xx_1}(x,z)=\frac{\Omega E_1}{3}\left(\begin{vmatrix} A_1<c> & J_1 \\ M_c & I_1 \end{vmatrix}+z\begin{vmatrix} A_1 & A_1<c> \\ J_1 & M_c \end{vmatrix}\right)\cdot\begin{vmatrix} A_1 & J_1 \\ J_1 & I_1 \end{vmatrix}^{-1}-\frac{1}{3}cE_1\Omega \tag{30}$$

for the top layer,

$$\sigma_{xx_2}(x,z)=\frac{\Omega E_2}{3}\left(\begin{vmatrix} A_1<c> & J_1 \\ M_c & I_1 \end{vmatrix}+z\begin{vmatrix} A_1 & A_1<c> \\ J_1 & M_c \end{vmatrix}\right)\cdot\begin{vmatrix} A_1 & J_1 \\ J_1 & I_1 \end{vmatrix}^{-1} \tag{31}$$

for the bottom layer, and

$$\frac{1}{\rho}=-\frac{\Omega}{3}\begin{vmatrix}A_1 & A_1<c>\\ J_1 & M_{c_1}\end{vmatrix}\begin{vmatrix}A_1 & J_1\\ J_1 & I_1\end{vmatrix}^{-1} \tag{32}$$

The radius of curvature is independent of the mechanical properties of each individual layer.

The stresses in the bilayer structure and the radius of curvature of the centroidal plane to the first-order approximation are

$$\sigma_{xx_1}(x,z)=\frac{\Omega E_1^2}{3}\left(\begin{vmatrix}A_1<c> & E_1J_1+E_2J_2\\ M_c & E_1I_1+E_2I_2\end{vmatrix}+z\begin{vmatrix}E_1A_1+E_2A_2 & A_1<c>\\ E_1J_1+E_2J_2 & M_c\end{vmatrix}\right) \tag{33}$$

$$\cdot\left(E_1^2A_1I_1+E_1E_2A_1I_2+E_1E_2A_2I_1-E_1^2J_1^2-2E_1E_2J_1J_2\right)^{-1}-\frac{1}{3}cE_1\Omega$$

for the top layer,

$$\sigma_{xx_2}(x,z)=\frac{\Omega E_1E_2}{3}\left(\begin{vmatrix}A_1<c> & E_1J_1+E_2J_2\\ M_c & E_1I_1+E_2I_2\end{vmatrix}+z\begin{vmatrix}E_1A_1+E_2A_2 & A_1<c>\\ E_1J_1+E_2J_2 & M_c\end{vmatrix}\right) \tag{34}$$

$$\cdot\left(E_1^2A_1I_1+E_1E_2A_1I_2+E_1E_2A_2I_1-E_1^2J_1^2-2E_1E_2J_1J_2\right)^{-1}$$

for the bottom layer, and

$$\frac{1}{\rho}=-\frac{\Omega E_1[(E_1A_1+E_2A_2)M_c-(E_1J_1+E_2J_2)A_1<c>]}{3\left(E_1^2A_1I_1+E_1E_2A_1I_2+E_1E_2A_2I_1-E_1^2J_1^2-2E_1E_2J_1J_2\right)} \tag{35}$$

3. Analyses of diffusion-induced bending of viscoelastic beams

Consider the diffusion-induced deformation in the framework of linear viscoelasticity. The relationship between the resultant strain tensor, $\boldsymbol{\varepsilon}_T$, and the diffusion-induced strain is

$$\boldsymbol{\varepsilon}_T=\boldsymbol{\varepsilon}+\frac{1}{3}c\Omega\mathbf{I} \tag{36}$$

which gives

$$\boldsymbol{\varepsilon}=\boldsymbol{\varepsilon}_T-\frac{1}{3}c\Omega\mathbf{I} \tag{37}$$

According to the theory of linear viscoelasticity [26], the differential form of three-dimensional constitutive relationship for viscoelastic materials is expressed as

$$P\left(\boldsymbol{\sigma}-\frac{\mathrm{tr}(\boldsymbol{\sigma})}{3}\mathbf{I}\right)=Q\left(\boldsymbol{\varepsilon}-\frac{\mathrm{tr}(\boldsymbol{\varepsilon})}{3}\mathbf{I}\right) \tag{38}$$

where P and Q are the following differential operators:

$$P=\sum_{k=0}^{m} a_k \frac{\partial^k}{\partial t^k} \quad \text{and} \quad Q=\sum_{k=0}^{n} b_k \frac{\partial^k}{\partial t^k} \tag{39}$$

with a_k and b_k being material constants.

Substituting Eq. (37) into Eq. (38), one obtains three-dimensional constitutive relationship for diffusion-induced stress in linear viscoelastic materials as

$$P\left(\boldsymbol{\sigma}-\frac{\mathrm{tr}(\boldsymbol{\sigma})}{3}\mathbf{I}\right)=Q\left(\boldsymbol{\varepsilon}_T-\frac{\mathrm{tr}(\boldsymbol{\varepsilon}_T)}{3}\mathbf{I}-c\Omega\mathbf{I}\right) \tag{40}$$

which together with equilibrium equations and boundary conditions can analyze the deformation behavior of linear viscoelastic materials due to diffusion/migration of solute atoms.

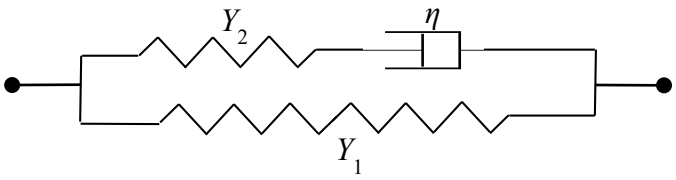

Figure 3. Schematic diagram of the Maxwell-type standard model

To understand the effect of viscoelastic behavior on the quasi-static bending of cantilever-based structures under the action of diffusion/migration of solute atoms, we focus on viscoelastic materials of the Maxwell-type standard model. The rheological behavior of the Maxwell-type standard model is described by two elastic elements with elastic moduli of Y_1 and Y_2, respectively, and a Newtonian element with viscosity of η, as shown in Fig. 3. Here the elastic element with the modulus of Y_2 is in series connection with the Newtonian element. From Fig. 3, the stress-strain relationship can be expressed as

$$\sigma=\sigma_1+\sigma_2 \tag{41}$$

$$\sigma_1=\frac{1}{Y_1}\left(\varepsilon-\frac{1}{3}c\Omega\right) \quad \text{and} \quad \left(\qquad \eta \right. \tag{42}$$

where σ is the total stress, ε is the total strain, σ_1 and σ_2 are the stresses applied to the elastic elements of Y_1 and Y_2, respectively. Define the Laplace transform of the stress, strain and concentration as

$$[\tilde{\quad} \quad \tilde{\quad} \quad z,t),\varepsilon(z,t),c(z,t)]e^{-st}dt \tag{43}$$

in which the s is a transform variable, and the wave-bar quantities indicate the Laplace transform. For the Maxwell-type standard model shown in Fig. 3, the stress-strain relationship in the

transform domain with the stress and strain being zero, respectively, at the instant of 0^- can be obtained as

$$\tilde{\quad} \qquad \tilde{\quad} \tag{44}$$

which gives

$$\tilde{I} \qquad \tilde{\quad} \cdot s\left(\frac{s}{Y_2}+\frac{1}{\eta}\right)^{-1} \tag{45}$$

Equation (45) is similar to the relationship used by Yang and Li [17] in the analysis of diffusion-induced beam bending in hydrogen sensors in the frame work of linear elasticity.

Using the correspondence principle, one can use the solution of an elastic problem to represent the solution of the corresponding viscoelastic problem in the transform domain by replacing the appropriate variables by their Laplace transform.

Viscoelastic beam of single layer

From Eqs. (11) and (12), the stress in the viscoelastic beam and the radius of curvature of the centroidal plane in the transform domain can be expressed as

$$\tilde{\quad} \qquad \tilde{\quad} \qquad \tilde{\quad} \tag{46}$$

$$L(\rho^{-1}) = -\frac{1}{3I}\tilde{M} \tag{47}$$

where $L(\cdot)$ is the Laplace transform. The inverse Laplace transform of Eq. (46) gives the stress in the viscoelastic beam as

$$\sigma_{xx}(x,z,t) = \frac{\Omega}{3}\int_0^t E(t-\xi)[(<c(x,z,\xi)> - c(x,z,\xi)) + \frac{z}{I}M_c(\xi)]d\xi \tag{48}$$

For viscoelastic materials of the Maxwell-type standard model, replacing the $\tilde{I}$ with the result in Eq. (45) and taking the inverse Laplace transform yield the stress in the viscoelastic beam as

$$\sigma_{xx}(x,z,t) = \frac{\Omega}{3}(Y_1+Y_2)\left([(<c(x,z,t)> - c(x,z,t)] + \frac{z}{I}\int_A (x,z,t)zdA\right) \tag{49}$$

$$-\frac{Y_2\Omega}{3}\cdot\frac{Y_2}{\eta}\int_0^t e^{-(t-\xi)Y_2/\eta}\left((<c(\xi)> - c(x,z,\xi)] + \frac{z}{I}\int_A c(x,z,\xi)zdA\right)d\xi$$

The inverse Laplace transform of Eq. (47) gives the radius of curvature of the centroidal plane as

$$\frac{1}{\rho} = -\frac{\Omega}{3I}\int_A c(x,z,t)zdA \tag{50}$$

Note that the results of (49) and (50) were obtained under the condition of $\int_A zdA = 0$ (i.e. the centroidal plane is the middle plane of the viscoelastic layer). It is evident that the radius of curvature of the centroidal plane is independent of the material properties of the viscoelastic beam of single layer. Equation (50) provides a simple approach to measure the coefficient of the volume expansion per mole of solute atoms from the bending of a viscoelastic beam under the condition that the mechanical properties of the viscoelastic beam is independent of the concentration of solute atoms.

Viscoelastic beam of bilayer with top layer being viscoelastic

Consider a bilayer structure with the top layer being viscoelastic and the bottom layer being elastic. There are no slip and separation between these two layers. Using the correspondence principle and Eq. (23), one obtains the radius of curvature of the centroidal plane of the viscoelastic beam of bilayer in the transform domain as

$$L(\rho^{-1}) = -\frac{\Omega \tilde{\quad}}{3}\Big|\tilde{\quad} \qquad E_2 A_2 \quad A_1 < \tilde{\quad} \qquad \tilde{\quad} \qquad \tilde{\quad} \qquad \tilde{\quad} \qquad (51)$$

Generally, one can use the inverse Laplace transform to obtain the solutions in the time domian from Eq. (51). However, the inverse Laplace transform of (51) is very complex, and one may not be able to obtain simple, closed-form solutions. The following only gives closed-form solutions with the zeroth-order approximation for two limiting cases.

Case I: Max(Y_1, Y_2)A_1<<E_2A_2 corresponding to the elastic bending of E_1A_1<<E_2A_2

For the problem corresponding to the elastic bending with E_1A_1<<E_2A_2, one can use the correspondence principle and Eq. (26) to obtain the radius of curvature of the centroidal plane in the transform domain to the zeroth-order approximation as

$$L(\rho^{-1}) = -\frac{\Omega \tilde{\quad} \qquad \tilde{\quad} \qquad \tilde{\quad} \qquad J_2}{3E_2 \qquad\qquad |J_2 \quad I_2|^{-1}} \qquad (52)$$

The inverse Laplace transform of Eq. (52) gives the temporal evolution of the radius of curvature of the centroidal plane of the viscoelastic beam of bilayer as

$$\frac{1}{\rho} = -\frac{\Omega}{3E_2}\int_0^t E_1(t-\xi)[A_2 M_c(\zeta) - J_2 A_1 < c(\xi) >]\,\mathrm{d}\xi \begin{vmatrix} A_2 & J_2 \\ J_2 & I_2 \end{vmatrix}^{-1} \qquad (53)$$

For viscoelastic materials of the Maxwell-type standard model, replacing $\tilde{I}$ in (52) with the result in Eq. (45) and taking the inverse Laplace transform yield the radius of curvature of the centroidal plane of the viscoelastic beam of bilayer as

$$\frac{1}{\rho} = -\frac{\Omega}{3E_2}\begin{vmatrix} A_2 & J_2 \\ J_2 & I_2 \end{vmatrix}^{-1} \left[(Y_1 + Y_2)[A_2 \int_{A_1} c(x,z,t) z dA - J_2 A_1 < c(x,z,t) >] \right. \tag{54}$$

$$\left. -\frac{Y_2^2}{\eta} \int_0^t e^{-(t-\xi)Y_2/\eta} \left(A_2 \int_{A_1} c(x,z,\xi) z dA - J_2 A_1 < c(\xi) > \right) d\xi \right]$$

Case II: $E_2A_2 << \text{Max}(Y_1, Y_2)A_1$ corresponding to the elastic bending of $E_2A_2 << E_1A_1$

For the problem corresponding to the elastic bending with $E_2A_2 << E_1A_1$, the radius of curvature of the centroidal plane in the transform domain to the zeroth-order approximation can be derived from Eq. (32) as

$$L(\rho^{-1}) = -\frac{\Omega}{3}\begin{vmatrix} A_1 & A_1 < \tilde{\ } & {}_1 \\ J_1 & \tilde{M} & I_1 \end{vmatrix}^{-1} \tag{55}$$

The inverse Laplace transform of Eq. (55) gives

$$\frac{1}{\rho} = -\frac{\Omega}{3}\begin{vmatrix} A_1 & A_1 < c(x,z,t) > \\ J_1 & \int_{A_1} c(x,z,t) z dA \end{vmatrix} \begin{vmatrix} A_1 & J_1 \\ J_1 & I_1 \end{vmatrix}^{-1} \tag{56}$$

which is independent of the materials properties of the viscoelastic beam.

4. Mass transport in a viscoelastic layer

Consider a viscoelastic layer with a rectangular cross-section. The dimensions of the viscoelastic layer in the *y*- and *z*-directions are much smaller than that in the *x*-direction, and the dimension in the *y*-direction is much smaller than that in *z*-direction. The diffusion equation (Fick's second law) for the diffusion/migration of solute atoms in the viscoelastic layer can be written as

$$\frac{\partial c}{\partial t} = D \frac{\partial^2 c}{\partial z^2} \tag{57}$$

with *D* being the diffusion coefficient of solute atoms in the viscoelastic layer. Under the condition that there is no solute atoms in the viscoelastic layer at time zero, the initial condition is

$$c(z,0) = 0 \tag{58}$$

There are two limiting types of boundary conditions; one is constant concentration on free surface, and the other is constant flux on free surface, which correspond to the potentiostatic and galvanostatic charging used in electrochemical measurement/cycling, respectively.

Case I: constant concentration on free surface

The free surface of the viscoelastic layer is exposed to a diffusing component which maintains a concentration of c_0 on that surface. The other surface is impermeable. The boundary conditions are

$$c\big|_{z=h} = c_0 \text{ and } \left.\frac{\partial c}{\partial z}\right|_{z=0} = 0 \qquad \text{for } t>0 \qquad (59)$$

The concentration distribution at any time t is

$$\frac{c}{c_0} = 1 - \frac{4}{\pi}\sum_{n=0}^{\infty}\frac{(-1)^n}{2n+1}\cos\left[\frac{(2n+1)\pi z}{2h}\right]\exp\left(-\frac{(2n+1)^2\pi^2 Dt}{4h^2}\right) \qquad (60)$$

which gives

$$M_c = -\frac{4bh^2c_0}{\pi^3}\sum_{n=0}^{\infty}\frac{(2n+1)\pi - 4(-1)^n}{(2n+1)^3}\exp\left(-\frac{(2n+1)^2\pi^2 Dt}{4h^2}\right) \qquad (61)$$

with the condition of $\int_A zdA = 0$ (i.e. the centroidal plane is the middle plane of the viscoelastic layer), and

$$M_c = \frac{bh^2c_0}{2}\left[1 - \frac{16}{\pi^3}\sum_{n=0}^{\infty}\frac{(2n+1)\pi - 2(-1)^n}{(2n+1)^3}\exp\left(-\frac{(2n+1)^2\pi^2 Dt}{4h^2}\right)\right] \qquad (62)$$

without the condition of $\int_A zdA = 0$. Here, b is the dimension in the y-direction, and h is the layer thickness.

The average concentration in the viscoelastic layer is calculated from Eq. (60) as

$$\frac{<c>}{c_0} = 1 - \frac{8}{\pi^2}\sum_{n=0}^{\infty}\frac{1}{(2n+1)^2}\exp\left(-\frac{(2n+1)^2\pi^2 Dt}{4h^2}\right) \qquad (63)$$

Case II: constant flux on free surface

The free surface of the viscoelastic layer is exposed to a diffusing component which maintains a constant flux of j_0 on that surface. The other surface is impermeable. The boundary conditions are

$$\left.\frac{\partial c}{\partial z}\right|_{z=h} = \frac{j_0}{D} \text{ and } \left.\frac{\partial c}{\partial z}\right|_{z=0} = 0 \qquad \text{for } t>0 \qquad (64)$$

The concentration distribution at any time t is

$$\frac{c}{j_0}=\frac{h}{D}\left[\frac{Dt}{h^2}+\frac{3z^2-h^2}{6h^2}-\frac{2}{\pi^2}\sum_{n=1}^{\infty}\frac{(-1)^n}{n^2}\cos\frac{n\pi z}{h}\exp\left(-\frac{n^2\pi^2 Dt}{h^2}\right)\right] \tag{65}$$

which gives

$$M_c=\frac{bj_0h^3}{D}\left[\frac{1}{24}-\frac{2}{\pi^4}\sum_{n=1}^{\infty}\frac{1-(-1)^n}{n^4}\exp\left(-\frac{n^2\pi^2 Dt}{h^2}\right)\right] \tag{66}$$

with the condition of $\int_A zdA=0$ (i.e. the centroidal plane is the middle plane of the viscoelastic layer), and

$$M_c=\frac{bj_0h^3}{D}\left[\frac{Dt}{2h^2}+\frac{1}{24}-\frac{2}{\pi^4}\sum_{n=1}^{\infty}\frac{1-(-1)^n}{n^4}\exp\left(-\frac{n^2\pi^2 Dt}{h^2}\right)\right] \tag{67}$$

without the condition of $\int_A zdA=0$.

The average concentration in the viscoelastic layer is calculated from Eq. (65) as

$$\frac{<c>}{j_0}=\frac{t}{h} \tag{68}$$

which is proportional the diffusion time.

5. Numerical calculation and discussion

Numerical results for the deflection of viscoelastic beams of retangular cross-sections are presented here. Considering that Au is chemically inert, we use Au film as the elastic layer in viscoelastic bilayer-structures, in which the widths of the Au layer and viscoelastic layer are same. The material for the viscoelastic layer is vinyl ester (VE) resins, since VE resins has potential applications in the construction of composite bipolar plate for electrochemical cells [27]. The solute atoms are water, and the molar volume of water is 18.03 mL/mol. The diffusion coefficient of water in VW resin is 7.04×10^{-8} cm^2/s [28]. Table 1 lists the materials properties used in the numerical calculations.

Table I: Materials properties ued in the numerical calculations

Material	E (GPa)	Y_1 (GPa)	Y_2 (GPa)	η (GPa·s)
Au	79			
VE resin [29]		2	0.8	150

Viscoelastic beam of single layer

For the viscoelastic layer of rectangular cross-section with the centroidal plane being the middle plane of the viscoelastic layer, there is

$$I = \frac{bh^3}{12} \tag{69}$$

Substituting Eqs. (61) and (66) in (50), respectively, and using Eq. (69), one obtains the radius of curvature as

$$\frac{1}{\rho} = \frac{16}{\pi^3}\frac{\Omega c_0}{h}\sum_{n=0}^{\infty}\frac{(2n+1)\pi - 4(-1)^n}{(2n+1)^3}\exp\left(-\frac{(2n+1)^2\pi^2 Dt}{4h^2}\right) \tag{70}$$

for the condition of constant concentration on free surface, and

$$\frac{1}{\rho} = -\frac{4\Omega j_0}{D}\left[\frac{1}{24} - \frac{2}{\pi^4}\sum_{n=1}^{\infty}\frac{1-(-1)^n}{n^4}\exp\left(-\frac{n^2\pi^2 Dt}{h^2}\right)\right] \tag{71}$$

for the condition of constant flux on free surface.

For $t\to\infty$, Eq. (71) reduces to

$$\frac{1}{\rho} = -\frac{1}{6}\frac{\Omega j_0}{D} \tag{72}$$

The radius of curvature for $t\to\infty$, is inversely proportional to the flux into the free surface.

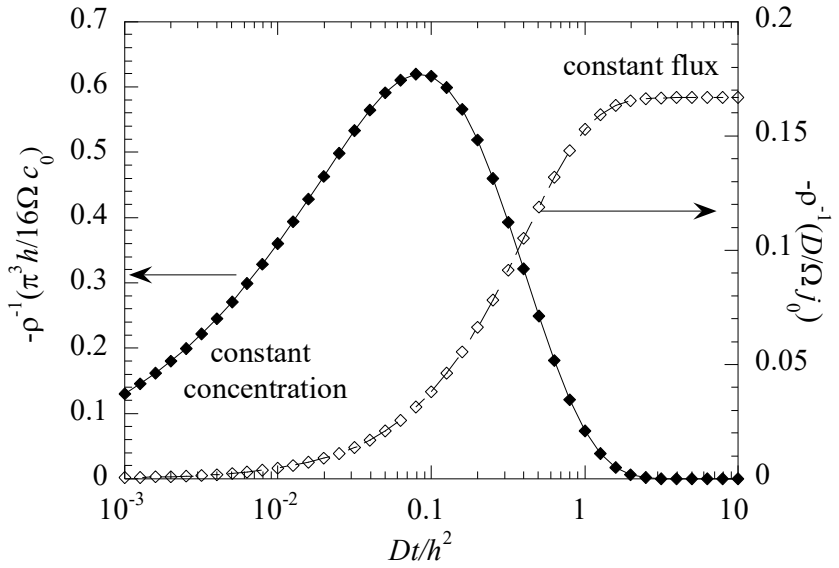

Figure 4. Temporal evolution of the radius of curvature of the viscoelastic beam of single layer induced by the diffusion/migration of solute atoms

Figure 4 shows the temporal variation of the radius of curvature induced by the diffusion/migration of solute atoms. For the condition of constant concentration on free surface,

the radius of curvature starts at infinity, decreases quickly to a minimum, and then increases gradually to infinity again when the solute atoms distribute uniformly in the viscoelastic beam. There is overshoot behavior in accord with that observed by Pei and Inganäs [13]. For the condition of constant flux on free surface, the radius of curvature starts at infinity and quickly decreases to constant (minimum) with the increase of the diffusion/migration time. There is a finite deflection as $t\to\infty$ in accord with the result given in Eq. (72). There is no overshoot behavior in contrast to the case with the condition of constant concentration on free surface. Such behavior reveals the effect of constant flux on the deflection of viscoelastic beams of single layer. The deflection of a viscoelastic beam of single layer is dependent on the boundary conditions.

Viscoelastic beam of bilayer with top layer being viscoelastic

Using the materials properties listed in Table I, one can calculate the temporal evolution of a viscoelastic beam of bilayer when subjected to different boundary conditions on free surface. For the viscoelastic layer of thickness h_1 and width b, the parameters of A_1, I_1 and J_1 are calculated as

$$A_1=bh_1,\ I_1=\frac{bh_1^3}{3}\ \text{and}\ J_1=\frac{bh_1^2}{2} \tag{73}$$

and for the elastic layer of thickness h_2 and width b, the parameters of A_2, I_2 and J_2 are found as

$$A_2=bh_2,\ I_2=\frac{bh_2^3}{3}\ \text{and}\ J_2=-\frac{bh_2^2}{2} \tag{74}$$

Substituting Eqs. (73) and (74) in Eq. (51) yields

$$L(\rho^{-1})=-\frac{\Omega\tilde{I}}{3}\left|\begin{matrix}\tilde{I}h_2 & h_1<\tilde{I}h_2 \\ \frac{\tilde{I}}{2}-\frac{}{2} & \frac{\tilde{I}}{2}-\frac{E_2h_2^2}{2}\end{matrix}\right|^{-1}\left|\begin{matrix}\frac{}{b} & \frac{\tilde{I}}{3}+\frac{}{3} \\ \frac{\tilde{I}}{2}-\frac{}{2} & \frac{\tilde{I}}{3}+\frac{}{3}\end{matrix}\right| \tag{75}$$

with

$$\tilde{I}\quad +s\left(\frac{s}{Y_2}+\frac{1}{\eta}\right)^{-1} \tag{76}$$

for the Maxwell-type standard model.

Case I: Max(Y_1, Y_2)A_1<<E_2A_2 corresponding to the elastic bending of E_1A_1<<E_2A_2

From Eq. (54), the radius of curvature of the centroidal plane of the viscoelastic beam of bilayer to the zeroth-order approximation is

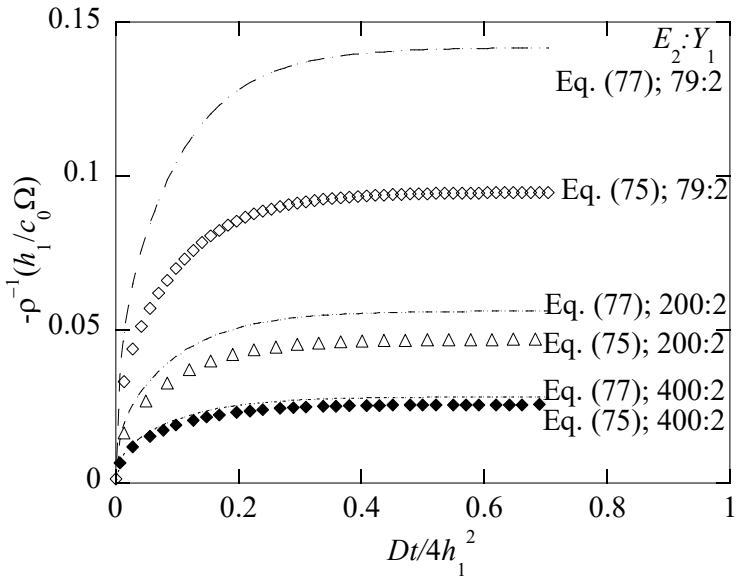

(a)

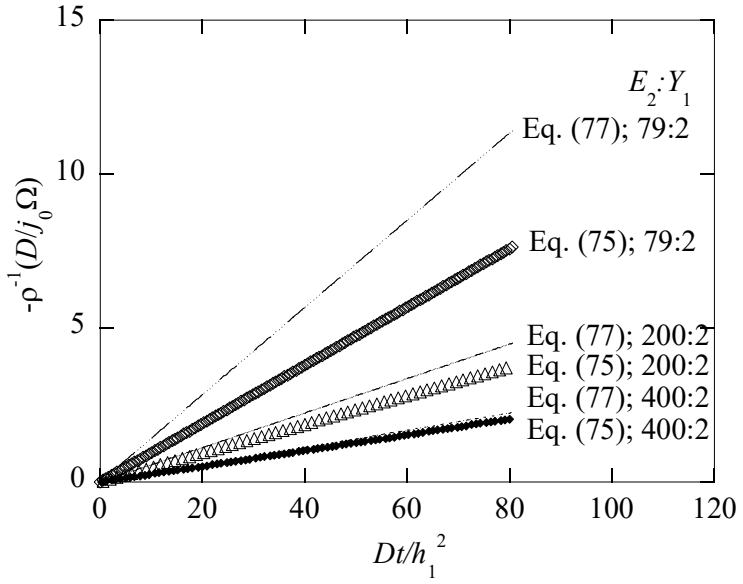

(b)

Figure 5. Temporal evolution of the radius of curvature of the viscoelastic beam of bilayer induced by the diffusion/migration of solute atoms with $Y_1A_1 < E_2A_2$ and h_1:h_2=50 nm: 50 nm; (a) constant concentration on free surface, and (b) constant flux on free surface

$$\frac{1}{\rho} = -\frac{4\Omega}{E_2 h_2^3}\left[(Y_1 + Y_2)[\int_0^{h_1} c(x,z,t)zdz + \frac{h_1 h_2}{2} < c(x,z,t) >] \right. \tag{77}$$

$$-\frac{Y_2^2}{\eta}\int_0^t e^{-(t-\xi)Y_2/\eta}\left(\int_0^{h_1} c(x,z,\xi)zdz+\frac{h_1h_2}{2}<c(\xi)>\right)d\xi\Bigg]$$

Using the materials properties given in Table I, the radii of curvature of the centroidal plane of the viscoelastic beam of bilayer for different ratios of E_2:Y_1 with h_1:h_2=50 nm: 50 nm and the condition of $Y_1A_1<E_2A_2$ ($Y_2<Y_1$) as a function of time are calculated by taking the inverse Laplace transform of Eq. (75). Figure 5 shows the calculation results. For comparison, the results calculated from Eq. (77) of the zeroth-order approximation are also included in Fig. 5. It is evident that the results calculated from Eq. (77) are in good accord with the results calculated from the inverse Laplace transform of Eq. (75) for large ratios of E_2A_2:Y_1A_1 for both two types of boundary conditions, i.e. constant concentration on free surface and constant flux on free surface. One can use Eq. (77) to calculate the radius of curvature of the centroidal plane of a viscoelastic beam of bilayer if the condition of $Y_1A_1<<E_2A_2$ is satisfied.

From Fig. 5a, one can note that the radius of curvature of the centroidal plane of the viscoelastic beam of bilayer with $Y_1A_1<E_2A_2$ starts at infinity and decreases to constant (minimum) in contrast to the case of the viscoelastic beam of single layer. There are no presences of overshoot and the relaxation to infinity of the radius of curvature of the centroidal plane for $t\rightarrow\infty$. Such behavior is likely due to the impermeability of the elastic layer to solute atoms, which allows the accumulation of solute atoms in the viscoelastic layer to cause the bending of the viscoelastic beam of bilayer. For $t\rightarrow\infty$, solute atoms are uniformly distributed in the viscoelastic layer, no further bending can occur.

It is interesting to note from Fig. 5b that the inverse of the radius of curvature of the centroidal plane of the viscoelastic beam of bilayer with $Y_1A_1<E_2A_2$ increases linearly with the diffusion/migration time in contrast to the result shown in Fig. 4 for the diffusion-induced bending of a viscoelastic beam of single layer. Such a difference can be attributed to the condition of $\int_A zdA=0$ for the viscoelastic beam of single layer (i.e. the centroidal plane is the middle plane of the viscoelastic layer). For viscoelastic beams of bilayer, $\int_{A_1} zdA+\int_{A_2} zdA\neq 0$ since there is no local strain directly introduced by solute atoms in elastic layer, as used in the analysis.

Case II: $E_2A_2<<\text{Max}(Y_1, Y_2)A_1$ corresponding to the elastic bending of $E_2A_2<<E_1A_1$

From Eq. (56), the radius of curvature of the centroidal plane of the viscoelastic beam of bilayer to the zeroth-order approximation is

$$\frac{1}{\rho} = -\frac{2\Omega}{h_1^3}\left(2\int_0^{h_1} c(x,z,t)zdz - h_1^2 < c(x,z,t) >\right) \tag{78}$$

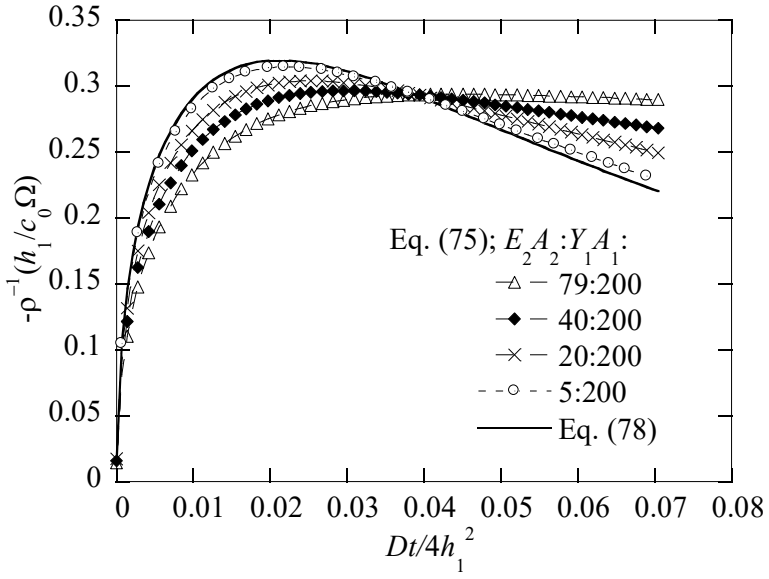

(a)

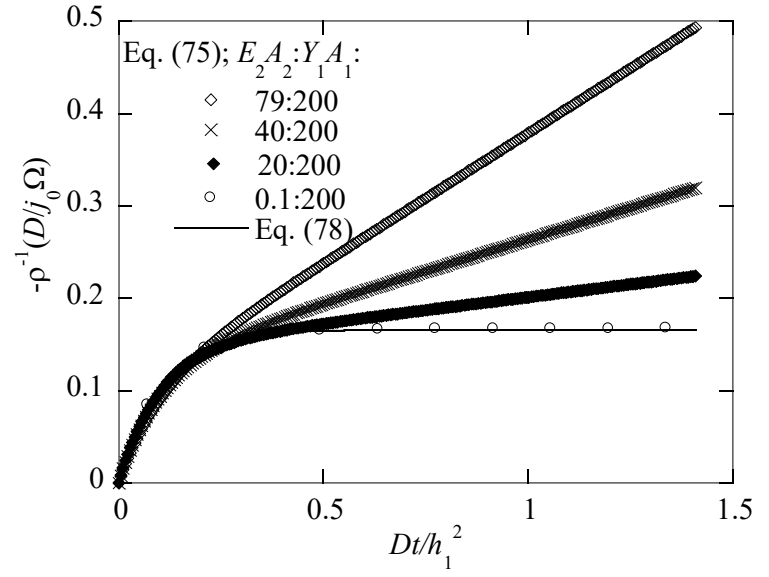

(b)

Figure 6. Temporal evolution of the radius of curvature of the viscoelastic beam of bilayer induced by the diffusion/migration of solute atoms with $E_2A_2<Y_1A_1$ (h_1:h_2=500 nm: 5 nm): (a) constant concentration on free surface, and (b) constant flux on free surface

The radii of curvature of the centroidal plane of the viscoelastic beam of bilayer for different ratios of E_2:Y_1 with h_1:h_2=500 nm: 5 nm and the condition of $E_2A_2<Y_1A_1$ ($Y_2<Y_1$) as a function of time are calculated by taking the inverse Laplace transform of Eq. (75), using the materials properties given in Table I. The calculation results are shown in Fig. 6, which also includes the results calculated from Eq. (78) of the zeroth-order approximation. The results calculated from Eq. (78) are in good accord with the results calculated from the inverse Laplace transform of Eq. (75) for large ratios of Y_1A_1:E_2A_2 for both two types of boundary conditions. Equation (77) can be used to analyze the deflection of viscoelastic beams of bilayer with one being elastic and the other being viscoelastic if the condition of $Y_1A_1<<E_2A_2$ is satisfied.

From Fig. 6a, one can note that, for relatively small ratio of Y_1A_1:E_2A_2 (>1), the radius of curvature of the centroidal plane of the viscoelastic beam of bilayer starts at infinity and decreases to constant (minimum) similar to the results shown in Fig. 5a with Y_1A_1:E_2A_2 (<1). There are no presences of overshoot and the relaxation to infinity of the radius of curvature of the centroidal plane for $t\rightarrow\infty$. This trend reveals the resistance of elastic layer to the bending of the viscoelastic beam of bilayer due to the impermeability of the elastic layer to solute atoms. The stiffer the elastic layer, the smaller is the deflection of the viscoelastic beam of bilayer. For relatively large ratio of Y_1A_1:E_2A_2 (>1), the radius of curvature of the centroidal plane of the viscoelastic beam of bilayer starts at infinity, decreases to constant (minimum), and then increases for the condition of constant concentration on free surface, which is similar to the case of the viscoelastic beam of single layer. There is overshoot of the radius of curvature of the centroidal plane. This result suggests that diffusion-induced overshoot of viscoelastic beams of bilayer with compliant elastic layer can occur due to less resistance to the beam bending.

According to Fig. 6b, the inverse of the radius of curvature of the centroidal plane of the viscoelastic beam of bilayer with $E_2A_2<Y_1A_1$ first increases nonlinearly with the increase of the diffusion/migration time of solute atoms and then becomes a linearly increasing function of the diffusion/migration time of solute atoms. The continuous diffusion/migration of solute atoms into the viscoelastic layer causes the decrease of the radius of curvature of the centroidal plane of the viscoelastic beam of bilayer.

6. Summary

The performance and sensitivity of cantilever-based sensors are dependent on the deflection/bending of the cantilever-based structures induced by the change of surface

stress/energy due to surface adsorption and/or by the diffusion/migration of solute atoms into the active layer. The work presented here has attempted to bring out the importance of the elastic layer and the boundary conditions for the diffusion/migration of solute atoms in understanding the deflection/bending of the cantilever-based structures consisting of a viscoelastic layer.

Using the Bernoulli–Euler assumption that planar sections perpendicular to the axis remain planar after bending, the exact solutions of the stress and the radius of curvature of the centroidal plane of an electric beam of bilayer have been derived from the elastic theory of diffusion-induced stress, in which solute atoms can only diffuse/migrate into the top layer. Both the stress and the radius of curvature are dependent on the average concentration of solute atoms and the diffusion moment.

The elastic theory of diffusion-induced stress is extended to the linear viscoelastic theory by considering the contribution of the diffusion-induced strain to the total strain. Three-dimensional constitutive relationship for diffusion-induced stress in linear viscoelastic materials is proposed. Using the correspondence principle between linear viscoelasticity and linear elasticity and the results from the diffusion-induced bending of elastic beams, the radii of curvature of the centroidal plane of the viscoelastic beams of single layer and bilayer with the top layer being viscoelastic in the transform domain are obtained.

For a viscoelastic beam of single layer, closed-form solution of the radius of curvature of the centroidal plane is derived. The radius of curvature of the centroidal plane is independent of the material properties of the viscoelastic beam. For the condition of constant concentration on free surface, there is overshoot behavior, and the radius of curvature starts at infinity, decreases quickly to a minimum, and then increases gradually to infinity again when the solute atoms distribute uniformly in the viscoelastic beam. For the condition of constant flux on free surface, there is no overshoot behavior, and the radius of curvature starts at infinity and quickly decreases to constant with the increase of the diffusion/migration time.

For a viscoelastic beam of bilayer with top layer being the Maxwell-type standard model, closed-form solutions of the radius of curvature of the centroidal plane to the zeroth-order approximation are derived. The numerical results show the presence of the overshoot behavior for very compliant elastic layer ($E_2A_2 << \mathrm{Max}(Y_1, Y_2)A_1$) under the condition of constant concentration on free surface. For relatively stiff elastic layer, there is no overshoot behavior under the condition of constant concentration on free surface. The radius of the centroidal plane reaches constant

(minimum), corresponding to uniform distribution of solute atoms in the viscoelastic layer. Under the condition of constant flux on free surface, the radius of curvature of the centroidal plane generally decreases continuously with the increase of the diffusion/migration time.

Acknowledgment

This work is supported by the NSF through the grant CMMI-1634540, monitored by Dr. Khershed Cooper.

References:

1. M. J. Wenzel, F. Josse and S. M. Heinrich, *J Appl Phys*, 2009, **105**, 064903.
2. M. Kandpal, A. K. Bandela, V. K. Hinge, V. R. Rao and C. P. Rao, *ACS Appl Mater Inter*, 2013, **5**, 13448-13456.
3. D. Larsson, A. Greve, J. M. Hvam, A. Boisen and K. Yvind, *Appl Phys Lett*, 2009, **94**, 091103.
4. R. Raiteri, M. Grattarola, H.-J. Butt and P. Skládal, *Sensors Actuators B: Chem*, 2001, **79**, 115-126.
5. M. Godin, V. Tabard-Cossa, Y. Miyahara, T. Monga, P. Williams, L. Beaulieu, R. B. Lennox and P. Grutter, *Nanotechnology*, 2010, **21**, 075501.
6. K. Ueno and M. Seo, *Journal of The Electrochemical Society*, 1999, **146**, 1496-1499.
7. V. Tabard-Cossa, M. Godin, L. Beaulieu and P. Grütter, *Sensors Actuators B: Chem*, 2005, **107**, 233-241.
8. S. Sahu, J. Scarminio and F. Decker, *J Electrochem Soc*, 1990, **137**, 1150-1154.
9. G. Láng, M. Ujvári, F. Bazsó, S. Vesztergom and F. Ujhelyi, *Electrochim Acta*, 2012, **73**, 59-69.
10. T. A. Brunt, E. D. Chabala, T. Rayment, S. J. O'Shea and M. E. Welland, *J Chem Soc, Faraday Trans*, 1996, **92**, 3807-3812.
11. C. Barbero, M. Miras and R. Kötz, *Electrochim Acta*, 1992, **37**, 429-437.
12. C. Barbero, M. Miras, O. Haas and R. Kötz, *J Electrochem Soc*, 1991, **138**, 669-672.
13. Q. Pei and O. Inganäs, *Solid State Ionics*, 1993, **60**, 161-166.
14. U. Laudahn, S. Fähler, H. Krebs, A. Pundt, M. Bicker, U. v. Hülsen, U. Geyer and R. Kirchheim, *Appl Phys Lett*, 1999, **74**, 647-649.
15. X. Chen, K.-Z. Xing and O. Inganäs, *Chem Mater*, 1996, **8**, 2439-2443.
16. M. J. Wenzel, F. Josse, S. M. Heinrich, E. Yaz and P. Datskos, *J Appl Phys*, 2008, **103**, 064913.
17. F. Q. Yang and J. C. M. Li, *J Appl Phys*, 2003, **93**, 9304-9309.
18. F. Yang, *Langmuir*, 2012, **28**, 3449-3452.
19. H.-C. Hsueh, D. Chiang and S. Lee, *Journal of Materials Research*, 2011, **26**, 1392-1398.
20. G. A. Snook, P. Kao and A. S. Best, *J Power Sources*, 2011, **196**, 1-12.

21. M. E. Roberts, D. R. Wheeler, B. B. McKenzie and B. C. Bunker, *J Mater Chem*, 2009, **19**, 6977-6979.
22. S. Ghosh and O. Inganäs, *Adv Mater*, 1999, **11**, 1214-1218.
23. C. Peng, S. Zhang, D. Jewell and G. Z. Chen, *Prog Nat Sci*, 2008, **18**, 777-788.
24. V. Khomenko, E. Frackowiak and F. Beguin, *Electrochim Acta*, 2005, **50**, 2499-2506.
25. F. Q. Yang, *Mat Sci Eng a-Struct*, 2005, **409**, 153-159.
26. N. W. Tschoegl, *The phenomenological theory of linear viscoelastic behavior: an introduction*, Springer Science & Business Media, 2012.
27. M. S. Wilson and D. N. Busick, *Composite bipolar plate for electrochemical cells, US Patent US6248467*, 2001.
28. L. Lima Sobrinho, M. Ferreira and F. L. Bastian, *Mater Res*, 2009, **12**, 353-361.
29. A. Plaseied and A. Fatemi, *J Mater Sci*, 2008, **43**, 1191-1199.